AD-A117 157 ARMY MISSILE COMMAND REDSTONE ARSENAL AL RESEARCH D--ETC F/G 4/1
TURBULENCE ANALYSIS BY USE OF THE FAST FOURIER TRANSFORM,(U)
JUN 82 O M ESSENWANGER

UNCLASSIFIED NL

END
DATE FILMED
8-82
DTIC

18 JUN 1982

TURBULENCE ANALYSIS BY USE OF THE FAST FOURIER TRANSFORM (U)

OSKAR M. ESSENWANGER, Ph.D.
US ARMY MISSILE COMMAND
US ARMY MISSILE LABORATORY, RESEARCH DIRECTORATE
REDSTONE ARSENAL, ALABAMA 35898

1. INTRODUCTION

Standard techniques in the analysis of turbulence include constructing the spectrum of turbulence. In the last three decades most authors have produced the spectrum via the calculation of the autocorrelation function, Tukey (1) or Blackman and Tukey (2). This method disclosed(among other things)a distinct economy in electronic data processing compared with the determination of the coefficients of the Fourier series. In fact, the Fourier transform of the autocorrelation function is the power spectral density, or in short, the spectrum, e.g., Tennekes and Lumley (3), p. 214.

Later Cooley and Tukey (4) introduced the Fast Fourier Transform (FFT) by which spectral values are calculated from the amplitudes of the Fourier series with even less computer time than is used by the autocorrelation method. Thus, "canned" programs of the FFT can be found readily on modern electronic data processing systems while the "old-fashioned" technique via the autocorrelation function is fading away. Some investigators may tacitly accept the postulation that the results from the FFT provide a valid spectrum in the analysis of turbulence. This postulation is examined in the following study.

It will be demonstrated that the FFT can be utilized for turbulence analysis but with certain reservations. The main problem is the calculation of the slope of the spectrum for a longer data series and the scatter of the standardized squared amplitudes for the FFT. The latter may produce outliers which could bias the slope of the spectral density.

It will also be shown that readings of the Gill anemometer (u-v-w). at one-second time intervals produced features in agreement with turbulence theory.

Finally, the FFT implies that the turbulence fluctuations can be superimposed upon the "stationary" profile for simulation studies of Army missile systems.

2. TURBULENCE AND POWER SPECTRUM

The presence of turbulence requires that the energy $E(\dot{x})$ in the power spectral density of the one-dimensional velocity (e.g., the wind's u-component) decreases as a function of the (standardized) wave number k:

$$E(k) = \alpha\varepsilon^{2/3}\ k^{-5/3} \qquad [1]$$

This decrease follows the Kolmogorov-Obukhov-Corrsin hypothesis on isotropic turbulence in the inertial subrange; see Tennekes and Lumley (3), p. 266, Priestly (5), p. 61, Hinze (6), p. 194, etc. The Kolmogorov constant α and the dissipation ε (here a constant) are of secondary interest. The reader is referred to the quoted literature for more details on α and ε.

The relationship to the power spectral density L_j is:

$$L_j = \int_{k_1}^{k_2} A_j^2\ (k)\ dk = E(k) \qquad [2]$$

where the wave number $k = j/p$ and p is the basic period. Computation of the power spectral density via the autocorrelation function was introduced by Tukey (1), see also Blackman and Tukey (2) or Panofsky and Brier (7). Power spectrum and Fourier series are associated by:

$$L_j = A_j^2/2\sigma^2 \qquad [3]$$

the squared standardized amplitude of the j^{th} Fourier term; σ^2 is the variance.

In double logarithmic coordinates:

$$\ell n(L_j) = \text{const} - (5/3)\ell n\ k = \text{const} - b\ell n\ k \qquad [4]$$

This is a linear equation with slope $b = -5/3$. Thus, turbulence is different from white noise, a random process, whose spectral characteristic is:

$$\ell n\ L_j = \text{const} \qquad [5]$$

with fluctuations of Lj produced by random errors.

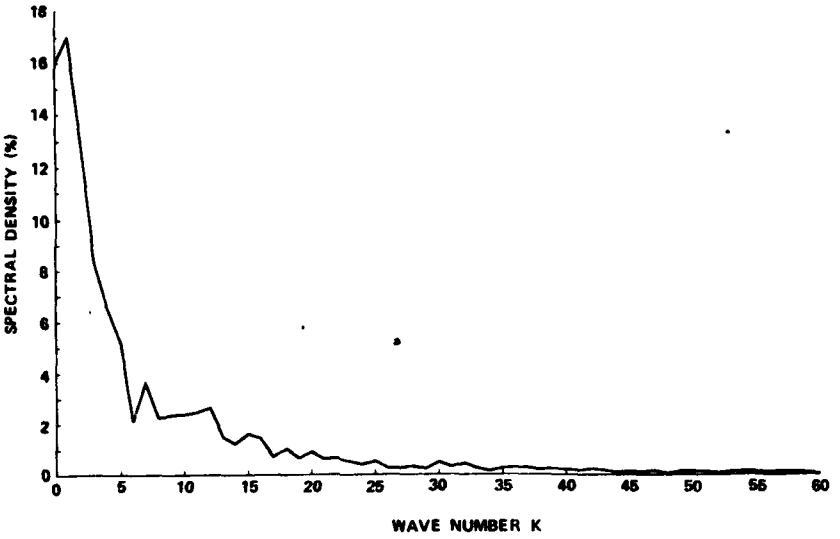

Fig. 1. Power spectrum of the windshear component Δu, 1-second recordings, 19 Aug 74. $\Delta u = u_2 - u_1$, level 2 at 9.1 m, level 1 at 5.5 m, maximum lag 60 seconds.

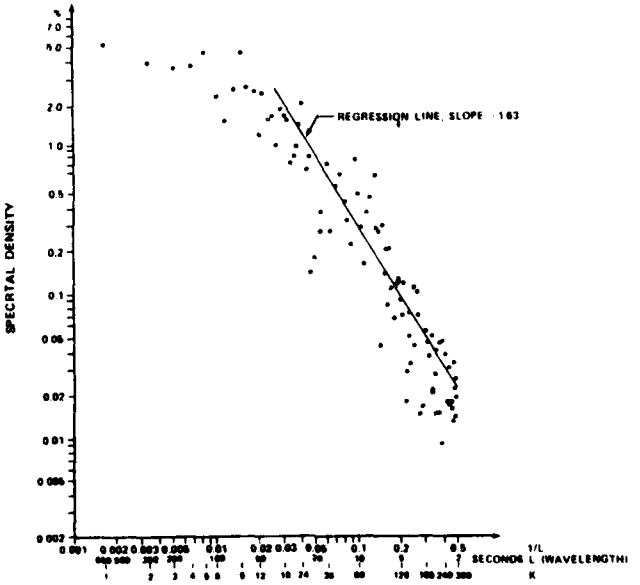

Fig. 2. Power spectrum for data of Figure 1 in double logarithmic coordinates. Maximum lag 300 seconds.

Fig. 1 illustrates the power spectrum for $\Delta u_i = u_{2i} - u_{1i}$ where the u_{ij} are the one dimensional wind components at level j of a meteorological tower. The data have been recorded on 19 August 1974 at one-second time intervals as measured by Gill anemometers (u-v-w), see Gill (8), Drinkrow (9) or Horst (10), on terrain of Redstone Arsenal, see Stewart (11), at 5.5 and 9.1 m height.

As illustrated by Fig. 1, the power spectrum density is not constant which excludes white noise as the generating background. A plot of the spectrum in double logarithmic coordinates (Fig. 2)* with maximum lag m = 300 seconds and calculation of the regression slope reveal that the major part of the spectral density follows almost a linear decline with slope b = -1.63 which is very close to -5/3.

The scatter of the data points is not too large, but deviations from the linear slope are found at low and high wave numbers. The deviations at low wave numbers are well known, e.g., Haugen (12) p.39, p. 169, Hinze (6) p. 203, Tennekes and Lumley (3) p. 270, Nicholls and Reading (13) Peterson (14) and others. Therefore, some authors use filters before turbulence analysis, e.g., Lester (15). The deviation in the region of high wave numbers may be caused by either nonisotropic turbulence such as described by Hinze (6) p. 501 or random noise at the low amplitudes L_j of the spectrum. Although the smoothed spectrum could have been plotted in Figure 2, the author selected to plot the unsmoothed spectral density values to display the scatter.

The computational effort of determining the slope of the regression line and the scatter of points can be reduced for the power spectrum by selecting a smaller maximum lag m. Figure 3 exhibits the spectral density as function of the wave number in double logarithmic coordinates for m = 60. The slope remains at -1.63 but the scatter is smaller than in Figure 2. As expected, the slope is independent of the maximum lag.

3. SPECTRAL DENSITY FROM THE FAST FOURIER TRANSFORM

Cooley and Tukey (4) have introduced the FFT as a technique for the rapid calculation of amplitudes of the Fourier series by electronic data processing. Since the power spectral density can be derived from these amplitudes, the FFT has replaced the Fourier transform of the autocorrelation function in many cases. The user of this substitution must be aware of some differences between these two analytical tools.

The autocorrelation function normalizes the reference of the phase angle of the Fourier terms and includes some smoothing of the data series.

* Only a selected number of spectral values have been plotted in Fig. 2 above wave number 60.

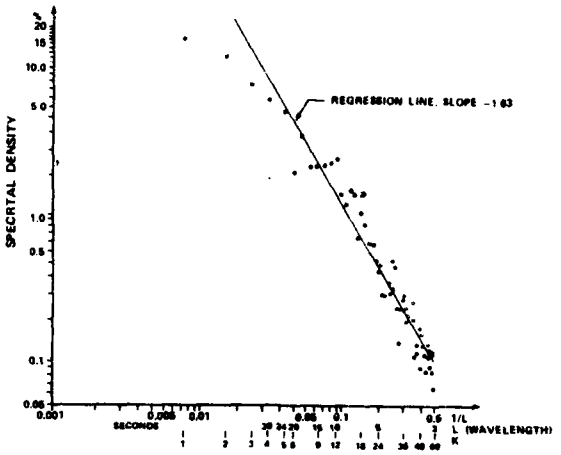

Fig. 3. Power spectrum for data of Figure 1 in double logarithmic coordinates. Maximum lag 60 seconds.

If the data contain "quasi-periodic" waves which appear intermittently, phase angle differences around π (i.e., 180^{o}) between previous and subsequent waves will lead to the diminution or extinction of the amplitude A in contrast to the Fourier transform of the autocorrelation function. This effect may produce some "outliers" in the spectral density of the FFT. Since the FFT is performed on the original data, the spectral amplitudes will also show a larger scatter (see later Figure 6).

The establishment of the power spectrum via the autocorrelation function provides for a choice of the maximum lag m which also determines the basic periods of the analysis. Thus, waves of long length (time cycle) can be lumped together in the wave number k = 0. As previously discussed, the slope is independent of the basic period in the spectrum.

In the FFT the basic period is identical with the length of the data N which also defines the maximum number of terms N/2 or (N-1)/2 whichever is a whole number. Shortening the length of the basic wave can only be accomplished by either truncation of the original data series or by averaging which may suppress waves of small length. Truncation of the autocorrelation function by selection of the maximum lag m is different.

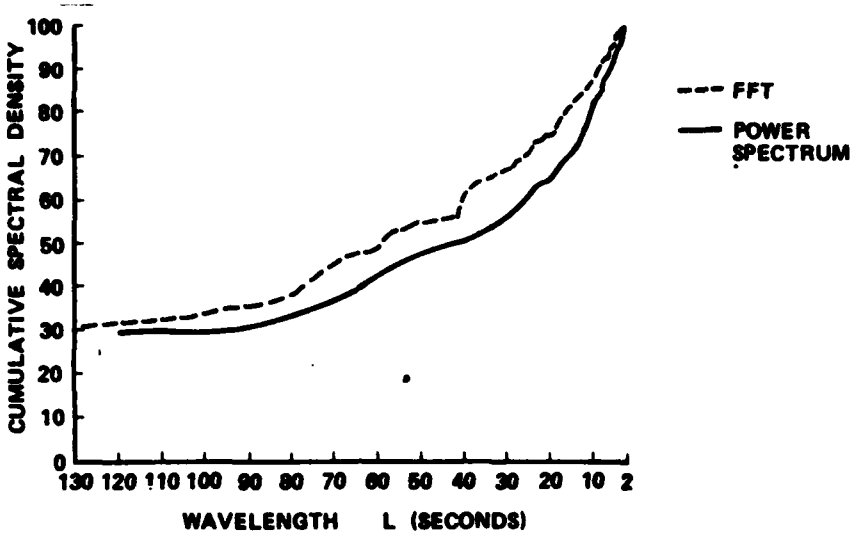

Fig. 4. Cumulative spectral density from autocorrelation (power spectrum) and from FFT for data of Figure 3.

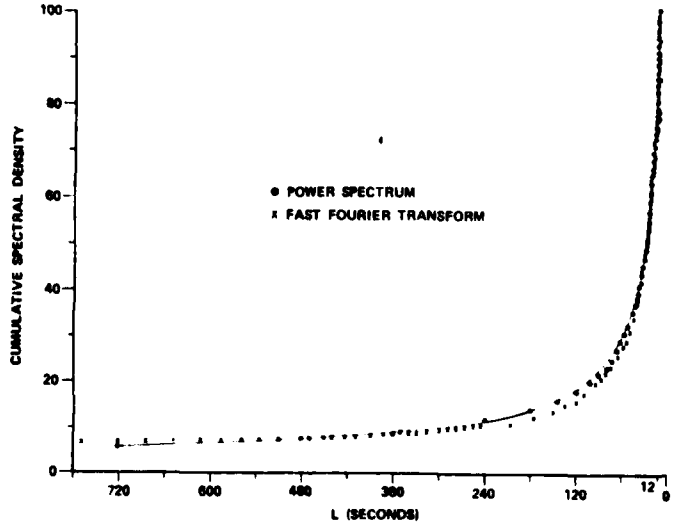

Fig. 5. Cummulative spectral density from autocorrelation (power spectrum) and FFT for data of 25 November 1981.

Consequently, it is no surprise that the cummulative spectral density obtained from the Fourier transform of the autocorrelation function and the FFT for the data of Fig. 2 or 3 exhibit some difference (Fig. 4). A disparity is not always found.

Fig. 5 exhibits the cumulative power spectral density of the Fourier transform spectrum and of the FFT for data recorded on 25 November 1981 at the AFGL Weather Test Facility at Otis AFB, Cape Cod, Massachusetts, measured with a Climatronic Wind Mark I System. As illustrated in this case, the result from the Fourier transform deviates only minimally from the one obtained by the FFT. Although the wave numbers (1-60) in both graphs (Fig. 4 and 5) are the same, the wave length (time cycle) is different because the data have been taken at 6-second intervals. In short, some spectra produced by the two tools may differ and others do not.

Fig. 6 provides the individual (squared and standardized) amplitudes calculated by the FFT for the same data as Fig. 2 and 3. The slope of the regression line b = -1.63 which is identical with the result from the

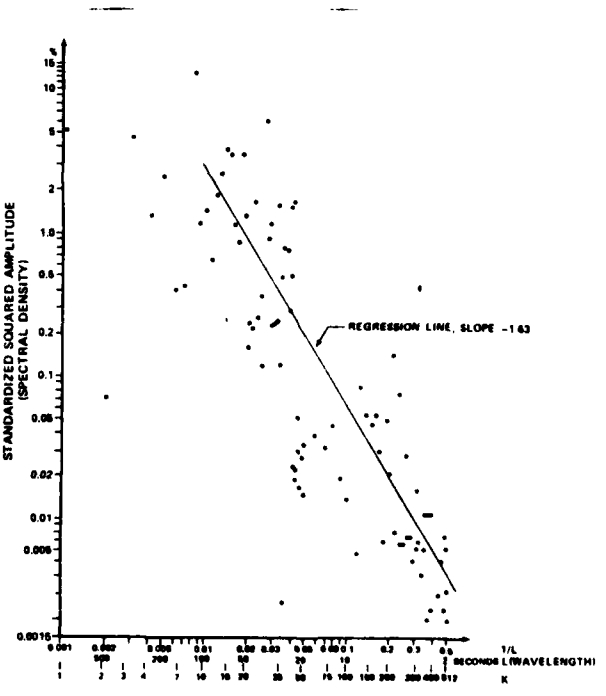

Fig. 6. Spectral density from FFT in double logarithmic coordinates, 19 August 1974 data.

power spectrum but b was not easily obtained. Spectral values of wave numbers with k over 400 and below 10 were truncated, which is equivalent to the application of a bandpass filter.

The weakness of the FFT is the disproportionate weight which high wave numbers have in the ordinary process of calculation of a regression line by least square methods and determination of its slope b. As outlined, the phase angle effect may produce some outliers which also could distort the value of the slope. Two methods are recommended to minimize the effect of disproportionate weight and outliers: truncation or median value regression.

Usually the truncation points (band pass filter) are not known a priori. Thus, they cannot be affixed for electronic data processing before computation of the regression line is made. An iterative truncation process is recommended starting with omitting one or two waves at low wave numbers (k = 1,2) and a multiple of waves with high numbers (e.g., for N/2 = 512, omit k=494 through 512). Then the residual variance and the slope are computed. The residual variance is:

$$v_R = \Sigma(Y_i - y_i)^2/N \qquad [6]$$

where Y_i is the analytical value of ℓnL_i from the regression line and y_i is ℓnL_i. The slope b will stabilize after some iterative steps; v_R will decrease.

The iterative process can be combined with a statistical evaluation of the slope b_j from iterative processes j by checking b_j against b_{j+1} or checking v_{R_j} against $v_{R_{j+1}}$. Test methods have been described by Anscombe (16) or Anscombe and Tukey (17).

The fitting of a regression line by ordinary least square methods may not eliminate the biasing effect of outliers, although after some stabilization of b_j and v_{R_j}, excessive deviations $|Y_i - y_i|$ could be omitted and the slope b recalculated. Although a threshold z could be determined and values $|Y_i - y_i| > |z|$ could be excluded, the procedure may be elaborate. A simple but robust method was suggested by Lawson (18) based on the median.

Lawson recommends the division of data into three sections, determining the median of y_i for the extreme sections, and then calculating the regression line from the two median values. This process is simple but may produce an uncertain statistical error. Therefore, for the FFT, this author suggests more than three sections depending on the data length N. An equal number of data in these individual sections is not required.

E.g., sections with a progressive number of data such as k=1-6, 7-18, 19-36, etc. may simultaneously resolve the problem of the excessive weight for waves with a high number of k. The regression line can be fitted to these median values. This reduces the somewhat lengthy process of iteration utilizing the N/2 Fourier coefficients.

It may be of interest to compare v_R for the data presented in Figures 2, 3, and 6 denoted v_{300}, v_{60}, and v_{FFT}, respectively. As expected v_{60} is smallest, $v_{60} = 0.089$. v_{300} is about 20% higher, $v_{300} = 0.108$. $V_{FFT} = 1.284$ which is 14 times higher than v_{60} but it is no surprise after examination of Figure 6 and comparing it with Figure 3.

In conclusion, the FFT can be utilized in turbulence analysis with some reservations and precautions. Furthermore, one-second recordings by Gill anemometers disclosed features in agreement with the turbulence hypothesis.

4. THE COMPOSITE WIND PROFILE

The evaluation of the wind effect upon missile systems sometimes requires a detailed wind profile in the microscale for short time intervals over the vertical coordinate. Unfortunately, these microscale observations are available only at special meteorological towers and seldom over 150 m. Thus, data sets must be prepared by analytical methods for simulation studies of missile systems. The results from the analysis presented in the preceding sections, especially in FFT, aid in the construction of these data sets.

It is well known that the wind profile as a function of altitude can be written as:

$$\vec{V}(h) = \vec{V}_s(h) + \vec{V}_t(h) \qquad [7]$$

where V_s represents the "stationary" part and V_t the small scale time and/or space fluctuations of the wind vector. In most cases, only the horizontal components are of importance or interest. Design data of the stationary part have been prepared for profiles of 1, 2 and 10 km by the author (19) at an earlier time. The author together with Billions (20) has also developed a methodology to separate the stationary and non-stationary part from special data measured by Reisig (21). From a power spectrum analysis of the data described by Essenwanger and Billions (20), the author could deduce that the fluctuations of the wind measurements in 15-m height intervals over the vertical range of 1 through 20 km were white noise. In contrast, the present investigations at ground level for a 4-m height difference reveal turbulence behavior of the Δu. Thus, the

author postulates from the tentative results that differences of the wind component in the lowest 1 or 2 km may follow turbulence structure rather than white noise, transforming to the latter above that range except in regions with known turbulence such as clear air turbulence. The study continues for confirmation of this postulation. We may now compose the u component for the wind from:

$$u(h) = u_s(h) + \Delta u\ (h) \qquad [8]$$

where $u_s(h)$ denotes the stationary part and:

$$\Delta u(h) = \sum_{j=k_1}^{k_2} A_j \sin\ (\alpha_{hj} + \beta_j) \qquad [9]$$

Here $\alpha_{hj} = j2\pi\ h/H$ where h is the altitude (h = 1,..., H).

In [9] the amplitudes A_j^2 follow the slope b = -5/3, i.e.,

$$2\ \ell n(A_k) = B-(5/3)\ \ell nk \qquad [10]$$

B is a constant to be explained below. The phase angles β_j are randomly distributed, i.e., β_j has a rectangular distribution. The waves $k < k_1$ may be considered as part of the stationary profile $u_s(h)$. The upper boundary is $k_2 \leq N/2$ or $k_2 \leq (N-1)/2$.

An equivalent formula is valid for the horizontal (rectangular) v(h) component of the wind.

Formulae [9] and [10] were utilized to simulate the fluctuations of Δu as a function of height (Figure 7). These fluctuations can be superimposed upon $u_s(h)$. This set of data should prove to be better suited for the evaluation of the small scale wind effect than the present technique of assuming a 95% wind profile and superimposing a 95% gust.

The investigations will continue with determination of numerical values for B. Theoretically an initial value can be found for k = 1. Then $B = \ell n(A_1^2)$, but it should be noticed that A_1 is not necessarily identical with the first Fourier term of the FFT as we learn from Figures 2, 3, and 6.

5. TIME AVERAGES AND DIFFERENCES OF WINDSPEED (MICRO-SCALE)

Common windspeed measurements (such as by ordinary cup anemometers) may be considered as time averages because of either a slow instrumental response time or a built-in time integration. In fact, this averaging is intended for conventional measurements to report a "representative" windspeed in synoptic observations. These measurements display a "meso-scale"

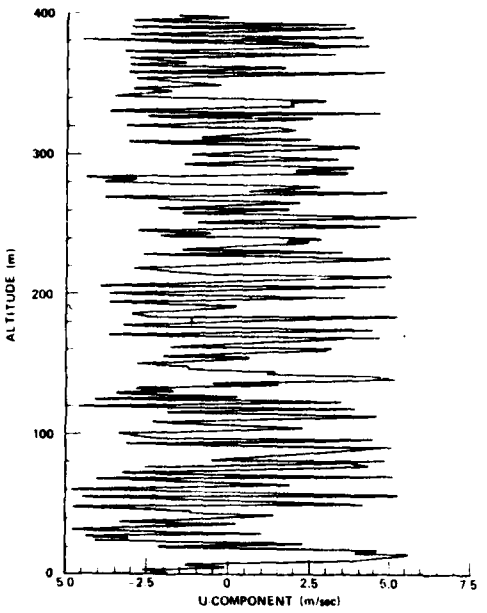

Fig. 7. Simulated data based on Eqns. [9] and [10].

of turbulence which was presented in the preceding sections. Seldom have attempts been made to relate the two phenomena, but a global evaluation (climatology) of turbulence as required for missile systems is difficult to establish without this important link. This short section serves to offer some solutions from preliminary data.

As previously outlined white noise (a random process for a sequence of independent data) produces a spectrum whose slope in eqn. [4] appears with $b \sim 0$. Persistence leads to $b < 0$. The structure of turbulence is reflected by producing $b = -5/3$. Red noise is another special form of persistence but the slope in the spectrum cannot readily be associated with a fixed numerical value. For smoothed data it may be $b \leq -2$ (Essenwanger and Reiter, 22).

The u and v components of the windspeed data measured on 19 August (see section 2) were subjected to an averaging process of the length 5, 10, 20, and 30 seconds and the spectrum calculated (FFT).

The slope for the u-component at the 5.5 m level appeared as $b = -2.8$ for the 10-second and -3.6 for the 20-second average. These numerical values imply a trend toward red noise.

Examination of the first autocorrelation reveals a drop from 0.97 for 1-second data to between 0.5 to 0.6 for the 30-second averages which indicates a looser connection between individual data of the sets. It is the structure of the autocorrelation, however, and not the first lag correlation which determines the link to red noise. As an example the sequence of the autocorrelation coefficients from lag 0 to lag 10 are exhibited for 1-second observations and 10-second averages (Table 1). Red noise requires:

$$r_i = (r_1)^i \qquad [11]$$

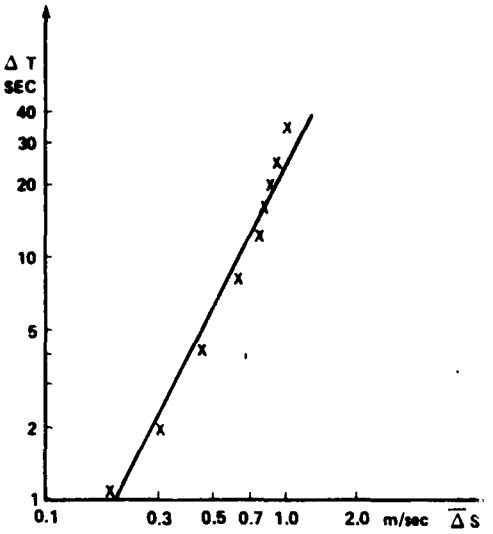

Fig. 8. Average windspeed $\overline{\Delta S}$ as function of time interval.

Table 1. Autocorrelation Function of u-component and Red Noise Autocorrelation Series

Lag	1-Sec.	Red N.	20-Sec.	Red N.
0	1.0	1.0	1.0	1.0
1	.974	0.974	.679	.679
2	.936	0.949	.459	.461
3	.900	0.924	.383	.313
4	.866	0.900	.272	.212
5	.836	0.877	.151	.144
6	.809	0.854	.103	.098
7	.785	0.832	.081	.065
8	.762	0.810	-.026	.045
9	.738	0.789	.028	.031
10	.715	0.768	.102	.021

which is identical with a first order Markov chain (Essenwanger, 23). We notice that the autocorrelation coefficients of 1-second data (u-component, level 5.5 m, 19 Aug. 74) drop more quickly than expected from red noise. In contrast, the autocorrelation coefficients for the 20-second averages are in line with expectations from red noise. The exceedance at lags 3 and 4 and the outlier at lag 8 seem to be associated with the presence of a quasi-cycle of around 2½ minutes during the 40-minutes when the data sample was taken on 19 Aug. 74.

Table 1 confirms the assumption of a red noise pattern in time averaged windspeeds. Thus, power spectra of conventional wind measurements could be interpreted as red noise. Reference to 1-second turbulence structure can then be achieved by determining the constants of eqn. [10] from the mid range of these spectra from "meso-scale" data rather than from fitting the first amplitudes (low k) as suggested for micro-scale turbulence data.

A second behavioral fact must be considered. Figure 8 displays the average difference of the windspeed $\overline{\Delta S}$ as a function of the time intervals ΔT, where:

$$\Delta S = [(\Delta u)^2 + (\Delta v)^2]^{\frac{1}{2}} \qquad [12]$$

Figure 8 discloses a linear relationship in the time range from

1 to 40 seconds differences with a slope of 0.5. Since the first 30 seconds were of primary interest here, the continuation of the data after the 40-second time interval is not shown, but it stabilizes at a constant value for longer time intervals. This result in micro-scale resembles earlier work by Neumann (24) who has demonstrated with customary wind data at the "meso-scale" for readings half an hour apart that the relative variability tends to a constant value as the time interval increases.

If the time structure as disclosed by Fig. 8 is not automatically met during the derivation of analytical data by eqn. [10], it may be necessary to find a solution to include the time structure on a vertical scale. This investigation is continuing.

The results for the 19 Aug 74 data sample were not completely conclusive, and further studies on data samples such as the 25 Nov 81 data will continue. However, one tentative result can be deduced. The numerical value of the slope in Figure 8 is 0.5. This is the same numerical value as derived for the windshear relationship for small intervals (Essenwanger and Reiter, 22, and Essenwanger, 25). Essenwanger and Reiter (22) could interpret the slope of 0.5 as a mixture between smoothed data and turbulence fluctuations. If this interpretation can be applied to the data of Fig. 8, a separation of the "stationary" and "non-stationary" part such as required in eqn. [7] is already the solution, and the time interval relation would implicitly appear.

6. CONCLUSION

The author has shown that the Fast Fourier Transform is a useful tool in turbulence analysis and the lack of "canned" programs of the Fourier transform of the autocorrelation function poses no serious problem. The user is cautioned, however, to be aware of the differences between the spectra produced by these two techniques.

A data sample procured with the Gill anemometer recorded at one-second time intervals reflect agreement with the turbulence hypothesis, (Fig. 2,3).

The FFT has the advantage that turbulence data can be readily expressed as a Fourier series. The amplitude relationship is expressed by eqns. [4] and [10] while the phase angles are randomly distributed. Although a set of phase angles can be constructed from random generators in electronic data processing, a simple technique would be a substitution from a set of empirical turbulence data.

The author has given an example of an analytically produced "non-stationary" set of data which could be superimposed on the "stationary" wind profile. These inferred data sets can be established where special

tower measurements are not available such as for altitudes beyond tower measurements and/or for geographic locations without tower measurements. These composed sets of wind data are better suited than present techniques for the assessment of the turbulence impact upon effectiveness, instrumental or missile sensitivity, and field use of systems such as DAFFR, Assault Breaker, CSWS, etc. by combining the "stationary" and "non-stationary" effect into one data set.

ACKNOWLEDGMENT

The author expresses his appreciation to Dr. Dorathy A. Stewart for her critical comments and the editorial review of the manuscript. Mrs. Alexa M. Mims deserves most of the credit for the preparation of the computer programs. My thanks go to Mr. Larry J. Levitt for his assistance in the preparation of the figures. The simulated data (Fig. 7) were prepared by Dr. Shi Tsan Wu. Finally, Mrs. Louise H. Cooksey deserves the credit for her patience and expeditious typing of the manuscript, and to CPT James C. Weyman, Air Force Geoph. Lab., for the special data of Fig.5.

REFERENCES

1. Tukey, J. W., 1949. The Sampling Theory of Power Spectrum Estimates. NAVEXOS-P-735, Woods Hole. Office of Naval Research, p. 47-67.

2. Blackman, R. B. and J. W. Tukey, 1958. The Measurement of Power Spectra. Dover Publ. Inc., New York, pp 190.

3. Tennekes, H., and J. L. Lumley, 1973. A First Course in Turbulence. MIT Press, Cambridge, Mass. pp 300.

4. Cooley and J. W. Tukey, 1965. An Algorithm for the Machine Calculation of Complex Fourier Series. Math. Comput. Vol. 19, p. 297-301.

5. Priestley, C. H. B., 1959. Turbulent Transfer in the Lower Atmosphere. University of Chicago Press, Chicago, pp 130.

6. Hinze, J. O., 1959. Turbulence, An Introduction to its Mechanism and Theory, McGraw Hill, New York, pp 586.

7. Panofsky, H. A. and G. W. Brier, 1958. Some Applications of Statistics to Meteorology. Pennsylvania State University, pp 224.

8. Gill, G. C., 1975. Development and Use of the Gill UVW Anemometer Boundary-Layer Meteorol., Vol. 8, p. 475-495.

9. Drinkrow, R., 1972. A Solution to the Paired Gill Anemometer Response Function. J. Appl. Meteorol., Vol. 11, p. 76-80.

10. Horst, T. W., 1973. Corrections for Response Errors in a Three-Component Propeller Anemometer. J. Appl. Meteorol., Vol. 12, p. 716-725.

11. Stewart, D. A., 1975. Turbulence Measurements from the Army Gas Dynamic Laser Range. US Army Missile Command Report RR-75-8, pp 25.

12. Haugen, D. A., 1973, editor. Workshop on Micrometeorology. Am. Meteor. Soc., Boston, pp 392.

13. Nicholls, S. and C. J. Readings, 1981. Spectral Characteristics of Surface Layer Turbulence Over the Sea. Qu. J. Roy. Meteorol. Soc. Vol. 107, p. 591-614.

14. Peterson, E. L., 1976. A Model for the Simulation of Atmospheric Turbulence. J. Appl. Meteorol. Vol. 15, p. 571-587.

15. Lester, P., 1972. An Energy Budget for Intermittent Turbulence in the Free Atmosphere. J. Appl. Meteorol., Vol. 11, p. 90-98.

16. Anscombe, F. J., 1967. Topics in the Investigation of Linear Relations Fitted by the Method of Least Squares. J. Roy. Stat. Soc., B, Vol. 29, p. 1-52.

17. Anscombe, F. J. and J. W. Tukey, 1963. The Examination and Analysis of Residuals. Technometrics, Vol. 5, p. 141-160.

18. Lawson, J. S., 1982. Application of Robust Regression in Designed Industrial Experiments. J. Qual. Techn., Vol. 14, p. 19-33.

19. Essenwanger, O. M., 1973. Wind Profile Parameters in the Ground Layer and Troposph. at Mid Latitudes. US Army Missile Comm.RR-73-6, pp 27.

20. Essenwanger, O. M. and N. S. Billi'ons, 1965. The Stationary and Non-Stationary Wind Profile. Pure and Appl. Geoph. Vol. 60, p. 160-166.

21. Reisig, G. H. R., 1956. Instantaneous and Continuous Wind Measurements up to the Higher Stratosphere. J. Meteorol. Vol. 13, p 448-455.

22. Essenwanger, O. M., and E. R. Reiter, 1969. Power Spectrum, Structure Function, Vertical Wind Shear, and Turbulence in Troposph. and Stratosph. Arch. Meteorol. Geoph. Bioklim, A, Vol. 18, p. 17-24.

23. Essenwanger, O. M., 1980. On Red Noise and Quasi-Periodicity in the Time Series of Atmospheric Temperature. Statistical Climatology, p. 165-181. Editors: S. Ikeda, E. Suzuki, E. Uchida and M. M. Yoshino. Elsevier, Amsterdam, pp 388.

24. Neumann, J. 1967. Wind Variability for Time Intervals of Medium Length. J. Appl. Meteor., Vol. 6, p. 587-589.

25. Essenwanger, O. M., 1963. On the Derivation of Frequ. Distrib. of Vector Shear Values for Small Shear Intervals. Geofis. Pura Appl. Vol 56, p. 216-224.


FILMED
8